Development 128, 3511-3520 (2001)
Printed in Great Britain © The Company of Biologists Limited 2001
DEV8808

Activity regulates programmed cell death of zebrafish Rohon-Beard neurons

Kurt R. Svoboda[1], Alicia E. Linares[1,2] and Angeles B. Ribera[1,2,*]

[1]Department of Physiology and Biophysics, University of Colorado Health Sciences Center, Denver, CO 80262, USA
[2]Program in Neurosciences, University of Colorado Health Sciences Center, Denver, CO 80262, USA
*Author for correspondence (e-mail: angie.ribera@uchsc.edu)

Accepted 22 June 2001

SUMMARY

Programmed cell death is a normal aspect of neuronal development. Typically, twice as many neurons are generated than survive. In extreme cases, all neurons within a population disappear during embryogenesis or by early stages of postnatal development. Examples of transient neuronal populations include Cajal-Retzius cells of the cerebral cortex and Rohon-Beard cells of the spinal cord. The novel mechanisms that lead to such massive cell death have not yet been identified.

We provide evidence that electrical activity regulates the cell death program of zebrafish Rohon-Beard cells. Activity was inhibited by reducing Na^+ current in Rohon-Beard cells either genetically (the *macho* mutation) or pharmacologically (tricaine). We examined the effects of activity block on three different reporters of cell death: DNA fragmentation, cytoskeletal rearrangements and cell body loss. Both the *mao* mutation and pharmacological blockade of Na^+ current reduced these signatures of the cell death program. Moreover, the *mao* mutation and pharmacological blockade of Na^+ current produced similar reductions in Rohon-Beard cell death. The results indicate that electrical activity provides signals that are required for the normal elimination of Rohon-Beard cells.

Key words: Programmed cell death, Rohon-Beard neurons, Zebrafish, Neural activity, Na^+ current, *macho* mutant

INTRODUCTION

Proper development and organization of the nervous system requires an extensive amount of programmed cell death (PCD; Cowan et al., 1984; Clark, 1985; Oppenheim, 1991). Perturbations that decrease neuronal PCD during embryogenesis result in malformations of the central nervous system (Kuida et al., 1996). By contrast, in the adult nervous system, PCD is less prominent, and, when present, is associated with neurodegenerative disorders. Deciphering the mechanisms that underlie neuronal PCD will contribute to our understanding of normal brain development as well as neurodegenerative disorders.

The zebrafish embryo provides several advantages for study of PCD in the developing vertebrate nervous system. At a gross level, the normal developmental changes that occur in neuronal morphology can be monitored in live embryos with a stereomicroscope. The optical transparency of the embryo allows easy visualization of dying cells in live embryos. In addition, a vast collection of DNA and antibody probes allows for more detailed examination of the consequences of cell death on pattern formation and neural differentiation (Metcalfe et al., 1990; Marusich et al., 1994). Furthermore, the feasibility of forward genetic approaches raises the possibility of identifying novel genes and mechanisms that contribute to neuronal PCD in the developing vertebrate nervous system.

During a recent large-scale mutagenesis screen of the zebrafish embryo, several mutations were identified that led to massive cell degeneration within the developing nervous system (Abdelliah et al., 1996; Furutani-Seiki et al., 1996; Daly and Sandell, 2000). The majority of mutations increased the extent of PCD via activation of a cell suicide program (apoptosis). In some instances, cell death was limited to a restricted region of the central nervous system, suggesting that early patterning defects were primary consequences of the mutations (Furutani-Seiki et al., 1996). A previously isolated mutant, *ned-1* (generated by γ-irradiation; Grunwald et al., 1988) led to massive neural cell death in most neurons, with the exception of early born primary neurons. Primary neurons, which include several populations of spinal neurons and the reticulospinal Mauthner cells, were spared and did not show enhanced cell death. The zebrafish neural degeneration mutations will aid in genetic dissection of the signals and biochemical pathways that are involved in neuronal PCD and ultimately pathological degenerative conditions.

Although the zebrafish neural degeneration mutants involve perturbations in cell death pathways that affect several neuronal populations, one interesting population appeared to be unaffected. This particular neuronal population, Rohon-Beard (RB) cells, normally undergo extreme PCD and exist only transiently in zebrafish as well as other teleost and amphibian species (Lamborghini, 1987; Hensey and Gautier, 1998; Reyes, 2000; Williams et al., 2000). By 5 days post fertilization (dpf), RB cells are completely eliminated from wild-type zebrafish (Henion et al., 1996; Reyes, 2000; Williams et al., 2000). Transient neuronal populations are not unique to fish and frog species, and are represented in

mammals by Cajal-Retzius cells of the cerebral cortex (Derer and Derer, 1990; Frotscher, 1997).

Despite the fact that all RB cells die during embryogenesis, no mutations have been isolated so far that prevent RB cell death. This is somewhat surprising, given the ease of studying RB cell differentiation and function. For example, RB cells are easy to recognize in live embryos using differential interference contrast optics (Grunwald et al., 1988) or in fixed preparations with a variety of immunological and molecular probes (Henion et al., 1996). In addition, their sensory function can be readily examined using a simple and rapid touch sensitivity test (Granato et al., 1996).

Although the zebrafish genetic mutants have not yet provided information regarding RB PCD, recent evidence suggests that neurotrophins are involved (Williams et al., 2000). Antibodies that block neurotrophin 3 (NT3) function increase the number of dying RB cells. Conversely, application of exogenous NT3 diminishes the extent of RB PCD. Withdrawal of neurotrophins can trigger cell death via a caspase-dependent pathway (Lievremont et al., 1999). Indeed, inhibition of caspases decreases the number of dying RB cells, indicating that PCD of RB neurons involves the activity of these proteolytic cell death enzymes (Williams et al., 2000).

Involvement of neurotrophins in RB PCD raises the possibility that neural activity also regulates the cell death pathway because activity affects expression and secretion of neurotrophins (Ghosh et al., 1994; Schinder and Poo, 2000). In addition, neural activity alters levels of intracellular Ca^{2+}, which can regulate cell death independently of neurotrophins (Larmet et al., 1992). No information exists about the role of activity in regulating cell death in the zebrafish nervous system.

We have examined the role that activity plays in the zebrafish embryo in RB cell death. Neural activity was perturbed either by use of a genetic mutant (*mao*) or a pharmacological blocker (tricaine). The *mao* mutant was isolated in a screen for motility mutants (Granato et al., 1996) and revealed by its insensitivity to tactile stimulation. Motor function appeared normal, suggesting that the deficit resides in mechanosensory neurons. Subsequent physiological examination indicated that the relevant mechanosensory neurons, RB cells, in *mao* mutants lacked voltage-gated Na^+ current and could not fire action potentials, thereby accounting for the behavioral deficit (Ribera and Nüsslein-Volhard, 1998). Tricaine is an anesthetic agent that preferentially blocks Na^+ current (Frazier and Narahashi, 1975; Wang et al., 1994). We found that block of Na^+ current, either genetically or pharmacologically, reduced RB cell death. Furthermore, the extents to which the *mao* mutation and tricaine treatment reduce cell death were similar. These results indicate that activity is required for the normal progression of cell death in RB cells.

MATERIALS AND METHODS

Embryo maintenance and drug treatment

The *mao* mutant line was kindly provided by Dr Hans-Georg Frohnhöfer of the Tübingen Stockcenter. The original ethynirosourea-induced mutation was created in fish of the Tü strain (Granato et al., 1996; Haffter et al., 1996). This line has been outbred for several generations with several wild-type strains and the behavioral phenotype persists in different genetic backgrounds (Granato et al., 1996; Ribera and Nüsslein-Volhard, 1998). The results reported here similarly did not depend upon the genetic background. We used three different wild-type strains for control studies (Tü, WIK and PS; the latter are fish from a local petstore); similar results were obtained with all three strains. Adults and embryos were housed at 28°C in a fish facility maintained in the UCHSC Center for Animal Laboratory Care. Embryos were developmentally staged according to previously described methods (Kimmel et al., 1995). 22-24 hpf embryos were manually dechorionated and transferred to Embryo Medium (EM; Westerfield, 1994) containing 0.002% 1-phenly-2 thiourea (PTU) to inhibit pigment formation. Tricaine treatment consisted of raising 24 hpf embryos at 28°C in EM-PTU containing 0.006% tricaine (ethyl 3-aminobenzoate, methansulfoninc acid; MS222; Sigma-Aldrich); controls were raised in EM-PTU at 28°C. Tricaine-treated and control fish were examined every 3 hours at room temperature to determine when the touch response was blocked in treated fish (typically by 30-32 hours post fertilization; hpf). Embryos received fresh embryo media (with the appropriate blockers, depending upon the experimental group) every 24 hours.

Immunocytochemistry

Embryos were fixed overnight at 4°C in 4% paraformaldehyde/phosphate-buffered saline containing 0.1% Tween-20 (PBST). Fixed embryos were washed and stored in PBST at 4°C. *mao* mutant embryos were identified on the basis of their touch insensitivity (Granto et al., 1996). Within a clutch of embryos, we clipped the tails of mutant or sibling embryos. The tail clipping allowed distinction of mutants from siblings (or wild type from tricaine-treated) while allowing them to be co-processed in the same reaction vial to ensure procedural consistency.

For immunocytochemical processing, embryos were first washed in PBST. Permeabilization was achieved by a 60 minute incubation in distilled H_2O, followed by a 20 minute exposure to 100% acetone at 4°C and a final 10-60 minute collagenase (1 mg/ml) treatment. Embryos were blocked for 1 hour in 10% normal calf serum/PBST and then incubated overnight at 4°C in 10% serum/PBST containing primary antibody. The primary antibodies anti-Hu (referred to here as HuAntibody, HuA; gift from Dr M. Marusich, University of Oregon), zn-12 (Developmental Hybridoma Bank, University of Iowa) and anti-acetylated tubulin (aat, Sigma-Aldrich) were used at 1:1000, 1:500 and 1:1000, respectively. The next morning, embryos were washed in PBST for at least 5 hours at room temperature and then incubated overnight (4°C) with a biotinylated, goat anti-mouse secondary antibody (Vector ABC Elite Kit, 1:250 dilution). Embryos were then washed in PBST for at least 2 hours and incubated in avidin/biotin (A/B) solution for 40 minutes. After the A/B incubation, embryos were washed in acetate buffer (50 mM, pH 5.0) for 2 hours. Embryos were then transferred to fresh acetate buffer solution containing 0.04% 3-Amino-9 Ethylcarbazol (AEC, Sigma-Aldrich) and 0.05% N,N-dimethyl-formamide (DMF, Sigma) in multi-well tissue culture dishes (see Kaplow, 1974). The chromogenic reaction was catalyzed by adding 0.01% H_2O_2 and stopped within 2-10 minutes by washing in PBST for at least 30 minutes.

Double-immunolabeling experiments were performed using the aat and zn-12 primary antibodies; the former recognizes a mature form of tubulin, whereas the latter binds to an extracellular sugar epitope on the plasma membrane (Metcalfe et al., 1990). The protocol described above was modified slightly and fluorescent secondary antibodies were used. Embryos were first incubated overnight with the zn-12 antibody (1:500). The next day, embryos were washed with PBST and then incubated overnight at 4°C in a biotinylated, goat anti-mouse secondary antibody (1:250, Vector ABC Elite Kit). On day 3, embryos were washed for 2-3 hours in PBST. To reveal zn-12 immunoreactivity, we applied rhodamine conjugated-streptavidin (Jackson ImmunoResearch, 1:400) for 5 hours at room temperature. After confirming positive zn-12 labeling, we washed embryos overnight at 4°C in PBST. On day 4, embryos were washed for 8-10 hours in PBST and then incubated with the aat primary antibody (1:1000) overnight at 4°C. On day 5, embryos were washed for 2

hours in PBST and then incubated in fluorescent secondary antibody (1:500, Alexa 488, Molecular Probes) at room temperature for 3-5 hours. Embryos were washed and stored in PBST (4°C) until examination. Similar results were obtained when the aat antibody was presented first and followed by the zn-12 antibody.

Detection of DNA fragmentation

Terminal transferase dUTP nick-end labeling (TUNEL) staining was combined with whole-mount immunocytochemistry as described previously (Reyes, 2000) with the following two modifications: proteinase K (1 μg/ml, Sigma Aldrich) treatment (37°C) was longer (45-60 minutes) and embryos were not cleared in glycerol.

Visualization of antibody labeling

Embryos that had been processed for aat immunoreactivity were squash-mounted laterally and viewed on an Eclipse TE200 inverted Nikon Microscope with a 20× or 40× objective and photographed using a Princeton Instruments digital camera. Images of embryos that were processed for both zn-12 and aat immunoreactivities were collected on a Nikon PCM-2000 laser-scanning confocal microscope and digital images were acquired at various focal planes.

For anti-Hu visualization, we embedded embryos dorsal side up in 1.25% low-melting point agarose (Gibco) and stored them in individual wells of tissue culture dishes until the RB neurons in each embryo were counted (see below). Each embryo was given a code designation so that cell counts could be made without knowledge of the embryo type (e.g. mutant versus sibling control). After cell counts had been performed, we mounted some embryos laterally to examine the dorsal root ganglia.

Analysis of Rohon-Beard somata number

Embryos were processed for immunocytochemistry and coded by one investigator, while another investigator counted RB somata. RB somata were identified on the basis of position and size in the spinal cord and strong HuA immunoreactivity. HuA recognizes an RNA binding protein that is expressed in several spinal cord neuron populations and abundantly in RB cells, as well as in the later appearing dorsal root ganglia (Marusich et al., 1994). RB somata were identified by their dorsal position, large size and intense HuA immunoreactivity (Grunwald et al., 1988; Henion et al., 1996; Ribera and Nüsslein-Volhard, 1998). The region that was analyzed extended from spinal cord segment 2 to the most caudal segment above the yolk sac extension. All data are presented as mean±s.e.m. Levels of statistical significance were assessed by an unpaired two-tailed Student's *t*-test. $P< 0.05$ was considered to be indicative of statistical significance.

RESULTS

Zebrafish embryos first display a response to tactile stimulation of the trunk at ~1 dpf (Grunwald et al., 1988; Saint-Amant and Drapeau, 1998; Saint-Amant and Drapeau, 2000). At this time, primary sensory neurons, known as RB cells, mediate the touch response in the trunk (Clarke et al., 1984; Soffe, 1991). One day later, dorsal root ganglion neurons begin to innervate the skin and thus potentially also contribute to the touch response. RB and dorsal root ganglion cells co-exist for a few days. By 5 dpf, however, all RB cells have been eliminated and dorsal root ganglion now solely mediate the touch response in the trunk (Reyes, 2000; Williams et al., 2000).

Development regulates the distribution of acetylated tubulin immunoreactivity in RB peripheral processes

We used whole-mount immunocytochemistry to monitor changes in the distribution of aat immunoreactivity as RB cells differentiate and die. Normal development and function of RB cells requires that they extend processes peripherally into the skin. The peripheral processes terminate in free endings that possess mechanosensitive channels, the site of the initial transduction event (Clarke et al., 1984). We examined the distribution of aat immunoreactivity during the period of maturation of RB peripheral processes (Fig. 1). In wild-type embryos, aat immunoreactivity was present in RB major peripheral processes at the time embryos first display an immediate response to tactile trunk stimulation (27 hpf). Between 27-36 hpf, aat immunoreactivity was continuous within the major peripheral process (Fig. 1A,B). As development progressed, the pattern of aat immunoreactivity changed. By 40 hpf, aat immunoreactivity became varicose rather than continuous (Fig. 1C). With further development, varicosities became more prevalent; none of the major peripheral processes exhibited the continuous, smooth aat immunoreactivity characteristic of earlier stages (Fig. 1D). At any given stage, aat immunoreactivity in peripheral processes was similar, regardless of their rostrocaudal position (data not shown).

The pattern of aat immunoreactivity within the spinal cord also changed during development. At 27 hpf, RB somata and early forming spinal tracts contained aat immunoreactivity. Nine and 13 hours later, aat immunoreactivity appeared more intense within spinal tracts. However, at 48 hpf, aat immunoreactivity within the spinal cord was substantially reduced. Only the beaded aat labeling of RB peripheral processes described above was obvious at 48 hpf.

In summary, between 27-48 hpf, the distribution of aat immunoreactivity changes in both RB major peripheral processes and the spinal cord. Thus, aat immunocytochemistry reflects aspects of RB cell differentiation that occur within the cytoskeleton of the peripheral processes.

Redistribution of acetylated tubulin immunoreactivity precedes retraction of RB peripheral processes

Recently, Williams et al. and Reyes demonstrated that zebrafish RB cells undergo massive programmed cell death (PCD) and are almost completely eliminated by 72 hpf (Williams et al., 2000; Reyes, 2000). At this time, all RB cells have retracted or are retracting their processes (Reyes, 2000). It is possible that redistribution of aat immunoreactivity into varicosities occurs as a result of process degeneration. However, process retraction is not prominent at 48 hpf (Reyes, 2000), a time when aat immunoreactivity already appears prominently as a collection of varicosities (Fig. 1D). To examine whether the formation of aat immunoreactive varicosities and process fragmentation occur simultaneously, we compared the distribution of aat to that of a cell surface glycoprotein recognized by the zn-12 monoclonal antibody (Metcalfe et al., 1990). RB peripheral processes of wild-type embryos were thus double-labeled for aat and zn-12 immunoreactivities. The zn-12 antibody revealed a complex network of peripheral processes (Fig. 2A). By contrast, aat immunoreactivity was restricted to the major peripheral processes (Fig. 2B). At 60 hpf, aat immunoreactivity in RB major peripheral processes was varicose (Fig. 2C, green), while zn-12 immunoreactivity appeared as a mesh of fine continuous fibers (Fig. 2C, red). In the major peripheral processes that exhibited both aat and zn-

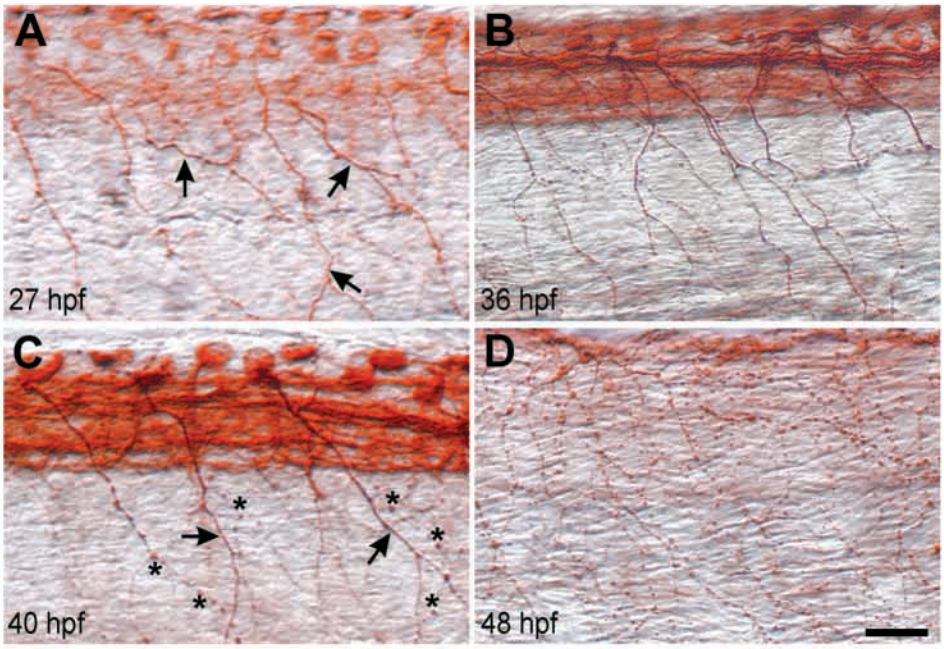

Fig. 1. Development regulates the distribution of anti-acetylated tubulin immunoreactivity in the peripheral processes of Rohon-Beard neurons. The distribution of aat in the major peripheral processes was examined using whole-mount immunocytochemistry (see Materials and Methods). The peripheral processes of RB cells were viewed in the focal plane of the skin of embryos that had been mounted laterally. In all views, anterior and dorsal are towards the left and upwards, respectively. (A) At 27 hpf, aat immunoreactivity displayed a uniform, continuous distribution (arrows) within the major peripheral processes of RB neurons. Within the spinal cord, aat immunoreactivity was present in emerging spinal tracts and RB somata. At this time, the embryo has just developed the ability to respond rapidly to tactile stimulation. (B) At 36 hpf, the distribution of aat immunoreactivity within peripheral processes remained continuous and uniform. In the spinal cord, aat immunoreactivity was more intense within spinal tracts when compared with spinal tracts of 27 hpf embryos. (C) By 40 hpf, aat immunoreactivity within peripheral processes began to display an altered distribution consisting of varicosities (asterisks). However, continuous, uniform labeling (arrows) was still evident in some processes. Within the spinal cord, aat immunoreactivity remained intense. (D) At 48 hpf, aat immunoreactivity was now only present as varicosities in the peripheral processes of RB cells. Within the spinal cord, aat immunoreactivity was no longer present. Scale bar: 20 μm.

12 immunoreactivities, aat immunoreactive varicosities were present. By contrast, zn-12 immunoreactivity in these processes was continuous, as would be typical of an intact process that had not yet fragmented. Similar findings were obtained from 48 hpf embryos (data not shown). These data indicate that redistribution of aat immunoreactivity precedes the fragmentation of processes and therefore is an earlier event in the program of RB cell death.

mao mutants do not display developmental regulation of anti-acetylated tubulin immunoreactivity

mao mutants do not respond to touch, although they can swim (Granato et al., 1996). In *mao* mutants, RB cells lack voltage-

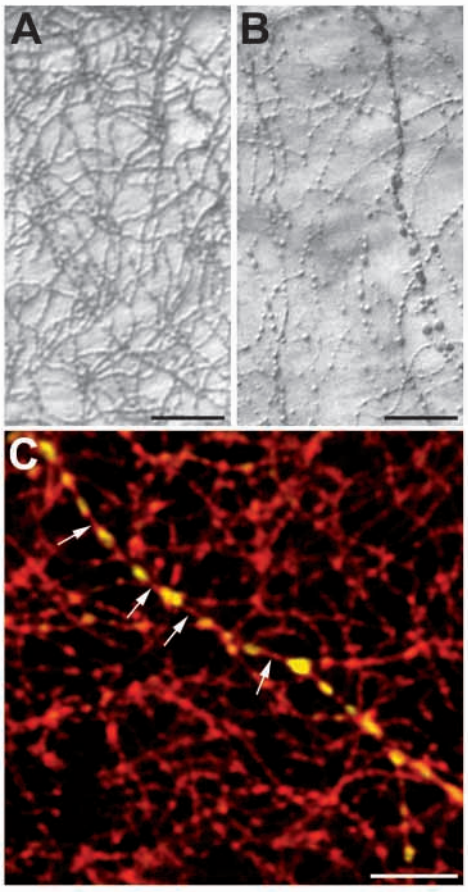

Fig. 2. Anti-acetylated tubulin immunoreactivity is distributed within varicosities of intact Rohon-Beard peripheral processes. (A) In a 60 hpf wild-type embryo, zn-12 immunoreactivity reveals the peripheral processes of RB cells are intact and form a mesh of fine fibers. (B) By contrast, aat immunoreactivity appears as discrete varicosities within a subset of the peripheral processes, referred to here as the major peripheral processes. (C) In double-antibody experiments, the peripheral processes of a 60 hpf embryo were co-labeled for aat (FITC, yellow) and zn-12 (Rhodamine, red) immunoreactivities. The former recognizes a mature form of tubulin, whereas the latter binds to an extracellular sugar epitope on the plasma membrane. Even though the peripheral processes appear intact at the level of the plasma membrane (red, arrows), aat immunoreactivity is found in only discrete subregions (yellow) of the peripheral processes, indicating that redistribution of aat immunoreactivity occurs before process fragmentation. Scale bars: 10 μm.

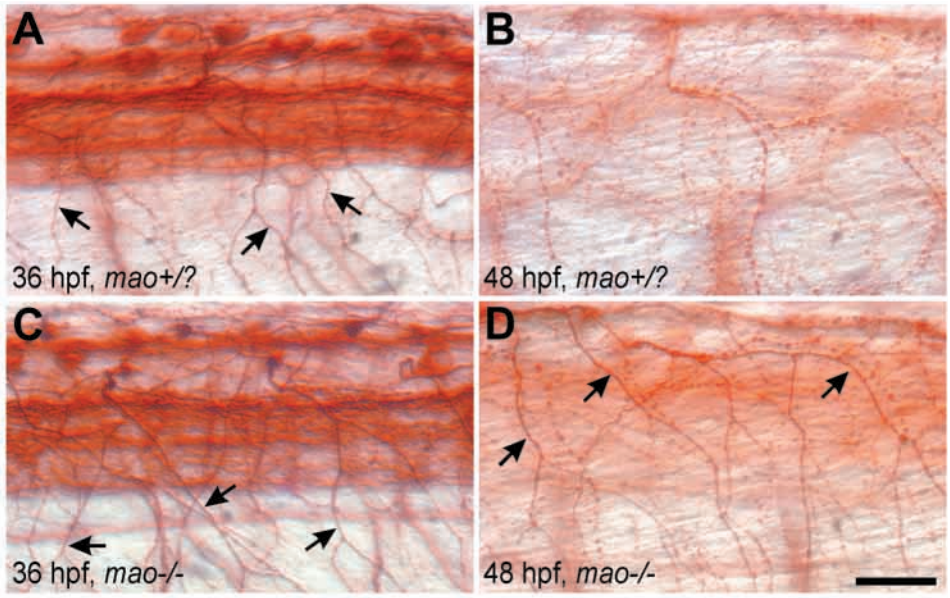

Fig. 3. Anti-acetylated tubulin immunoreactivity within Rohon-Beard peripheral processes differs between touch-insensitive *mao* mutant and sibling embryos at late but not early times. The peripheral processes of sibling control (A) and *mao* mutant (C) embryos displayed similar patterns of aat immunoreactivity (arrows) at the initial stages of touch sensitivity (compare with Fig. 1A,B). However, at 48 hpf, the pattern of aat immunoreactivity of *mao* mutants (D) differed from that of sibling controls (B) and resembles that observed at earlier stages in either sibling, mutant or wild-type embryos (Figs 3A,C, 1A,B). In all examples, images were taken from skin regions at caudal levels of the spinal cord. Scale bar: 20 μm.

gated Na^+ current and do not fire action potentials, thus accounting for the behavioral phenotype (Ribera and Nüsslein-Volhard, 1998). To examine the possibility that the *mao* mutation affects RB cell differentiation and/or death, we analyzed the distributions of aat immunoreactivity in RB peripheral processes and the spinal cord of *mao* mutant and sibling control embryos. At 36 hpf, no differences were noted in aat immunoreactivity between wild-type, *mao* mutant or sibling control embryos (compare Fig. 1B with Fig. 3A,C). However, at 48 hpf, the distribution of aat

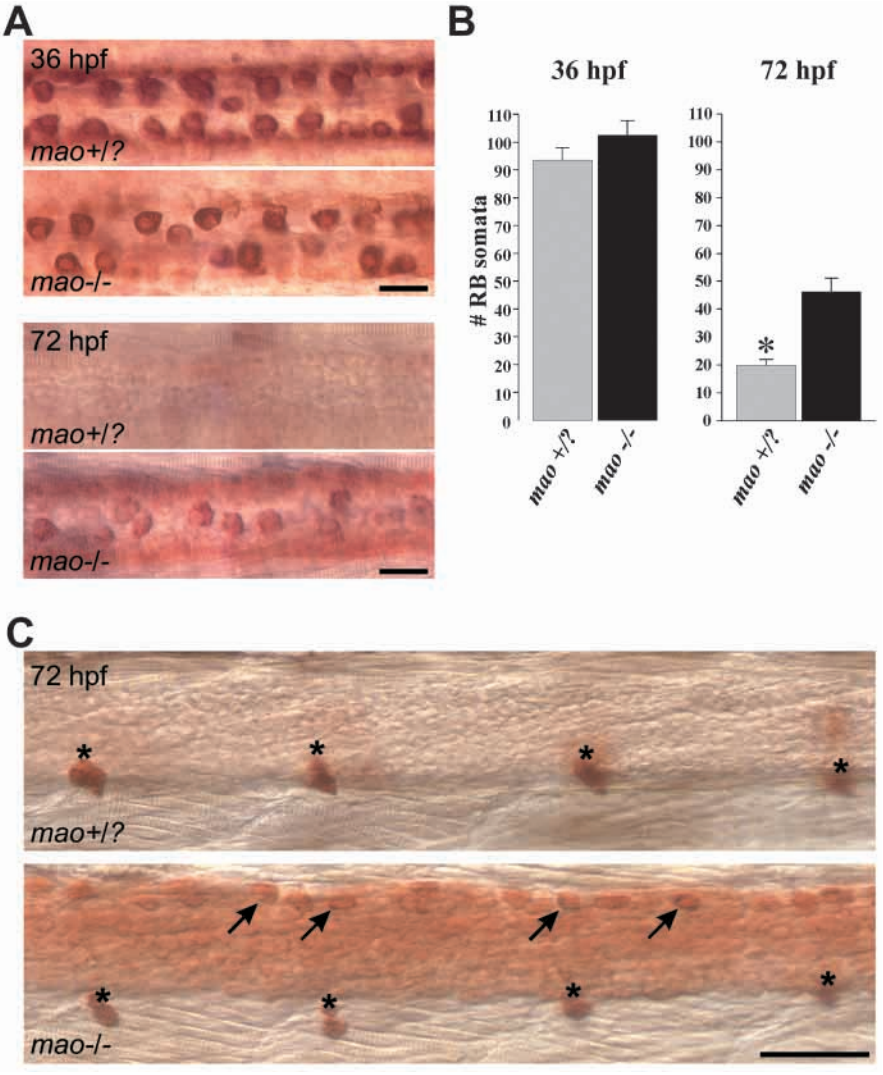

Fig. 4. The *mao* mutation diminishes the normal loss of Rohon-Beard cell bodies. (A) Dorsal views of two segments from 36 (top) and 72 (bottom) hpf *mao* mutant and sibling embryos that had been processed for HuA immunocytochemistry (see Materials and Methods). At 36 hpf, mutant and sibling embryos have similar numbers of RB somata. However, at 72 hpf, RB somata have been eliminated in the sibling but retained in the mutant embryo. (B) RB cell counts for *mao* mutant and sibling embryos at 36 (left) and 72 (right) hpf. Each column represents the mean±s.e.m. for data collected from eight to ten embryos. At 72 hpf, there are significantly more RB somata in mutants versus siblings (P<0.0001). (C) In lateral views of 72 hpf sibling and mutant embryos (top and bottom, respectively), dorsal root ganglia (asterisks) and any remaining RB cells (arrows) can be seen. In siblings, only the dorsal root ganglia are present. By contrast, mutants possess both dorsal root ganglia and RB cells. Scale bars: 20 μm in A; 40 μm in C.

immunoreactivity in RB peripheral processes of *mao* mutants differed dramatically from that of either sibling control or wild-type embryos (Figs 1D, 3). Specifically, in *mao* mutants, aat immunoreactivity in RB peripheral processes retained its continuous, smooth distribution (Fig. 3D). Aat immunoreactivity remained continuous in RB peripheral process of *mao* mutants as late as it was examined (72 hpf; data not shown).

Within the spinal cord, aat immunoreactivity did not differ between mutant and sibling embryos at any developmental stage. In all embryos, aat immunoreactivity was prominent in the spinal cord at 27-36 hpf but substantially reduced by 48 hpf.

Rohon-Beard cell development involves an extreme form of programmed cell death that is attenuated in *mao* mutants

Formation of aat immunoreactive varicosities in RB peripheral processes is suppressed in the *mao* mutant, raising the possibility that PCD is attenuated in *mao* mutants. Accordingly, we relied on RB morphology and HuA immunoreactivity to count RB somata at several stages during the normal period of RB cell elimination. HuA immunoreactivity also reveals dorsal root ganglia as they begin to appear (~48 hpf).

At 36 hpf, HuA immunoreactivity revealed little difference in the number of RB somata in *mao* mutants versus sibling embryos (Fig. 4A, top). Cell counts indicated that there was no significant difference in the number of RB somata between *mao* mutant and sibling embryos (Fig. 4B, left).

At 72 hpf, very few or no RB cells were present in sibling control embryos (Fig. 4A, bottom). However, in *mao* mutants, HuA immunoreactivity revealed the persistence of numerous RB cells. On average, twice as many RB cells were present in mutants compared with their sibling controls (Fig. 4B, right). By contrast, in both *mao* mutant and sibling embryos, HuA immunoreactivity is present in the dorsal root ganglia (Fig. 4C).

In addition to being molecularly unique cells, RB cells possess distinguishing morphological features (large soma, dorsal position) that permit their identification directly in fixed and live preparations of zebrafish embryos (Grunwald et al., 1988). Visualization of 72 hpf embryos with Hoffman optics indicates that RB cells are more numerous in *mao* mutant when compared with sibling embryos (Fig. 5). These data indicate that the *mao* mutation leads to a reduction in RB cell PCD.

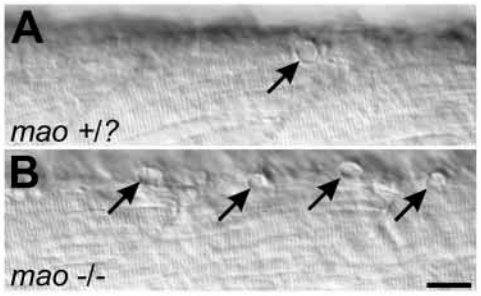

Fig. 5. Direct visualization of Rohon-Beard cells in *mao* mutant and sibling embryos. RB cells in *mao* sibling (A) and mutant (B) 72 hpf embryos were directly visualized with Hoffman optics. RB cells (arrows) are easily recognized on the basis of their dorsal position and relatively large size within the spinal cord (Grunwald et al., 1988). More RB cells are present in *mao* mutants than sibling embryos. Scale bar: 20 μm.

Mao mutants display early defects in programmed cell death

An early manifestation of entry into the PCD pathway is DNA fragmentation (Kerr et al., 1972; Searle et al., 1982). DNA fragmentation can be revealed in zebrafish using TUNEL staining (Reyes, 2000; Williams et al., 2000). At 36 hpf, wild-type embryos show a high incidence of positive TUNEL labeling in the RB cell population (Williams et al., 2000). In *mao* mutants, significantly fewer TUNEL-positive RB cells are present at 36 hpf compared with sibling control embryos (Fig. 6). Thus, *mao* mutants displayed attenuations in PCD at early (TUNEL), intermediate (redistribution of aat immunoreactivity in RB peripheral processes) and late (soma number) stages.

Pharmacological suppression of Na^+ current phenocopies the effect of the *mao* mutation on programmed cell death of Rohon-Beard cells

Our results indicate that the *mao* mutation reduced the extent of normally occurring RB PCD. The *mao* mutation leads to elimination of the majority of voltage-gated Na^+ current and suppression of action potentials in RB cells (Ribera and

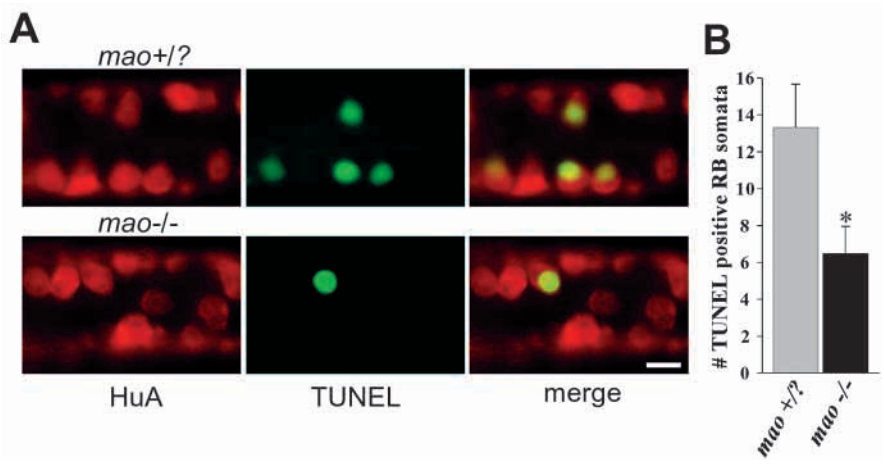

Fig. 6. The *mao* mutation diminishes an early sign of programmed cell death – DNA fragmentation. (A) *Mao* mutant (bottom) and sibling (top) 36 hpf embryos were co-processed for HuA immunocytochemistry (left) and TUNEL (middle; see Materials and Methods). In the merged images (right), fewer TUNEL-positive RB cells are present in the *mao* mutant versus the sibling embryo. Scale bar:10 μm. (B) Cell counts of TUNEL-positive RB neurons indicate that there are significantly fewer TUNEL-positive RB neurons in 36 hpf *mao* mutants compared with siblings ($P<0.05$; $n=4$ and $n=3$, mutants and siblings, respectively).

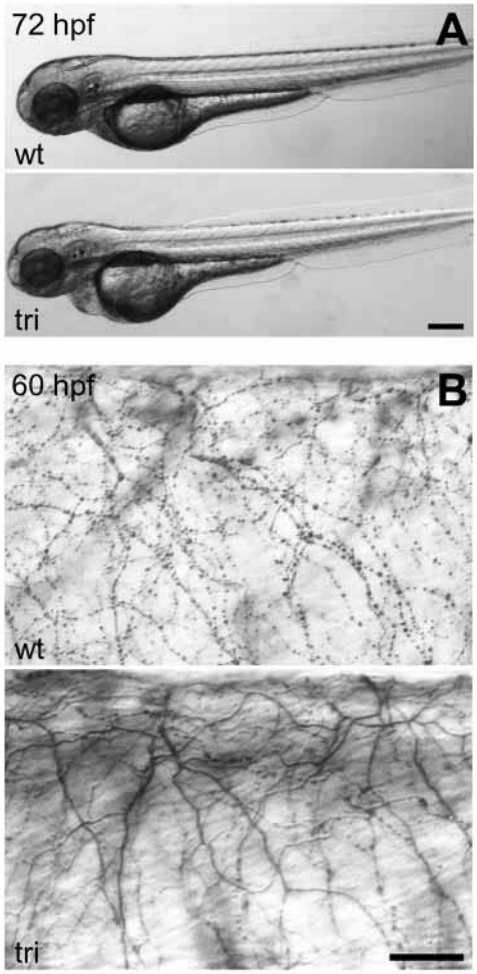

Fig. 7. Pharmacological block of neural activity phenocopies the effect of the *mao* mutation on Rohon-Beard peripheral processes. (A) Wild-type embryos were treated with 0.006% tricaine between 24-72 hpf. Untreated (top) and tricaine-treated (bottom) embryos develop normally without obvious gross morphological differences. Scale bar: 200 μm. (B) aat immunoreactivity in a 60 hpf wild-type (top) is present in varicosities, as found in *mao* sibling embryos of similar age (Fig. 3B; data not shown). By contrast, tricaine-treated embryos (bottom) do not develop aat-positive varicosities. Thus, tricaine-treatment phenocopies the effect of the *mao* mutation on RB peripheral processes (Fig. 3D). Scale bar: 20 μm.

Nüsslein-Volhard, 1998). The *mao* gene may directly and independently affect both RB cell Na^+ current and PCD. Alternatively, the *mao* mutation might directly control RB electrical activity, which in turn regulates PCD. To distinguish between these possibilities, we tested whether pharmacological suppression of Na^+ current would have effects on PCD similar to those of the *mao* mutation.

Embryos were placed in a low dose of tricaine (0.006%) at 24 hpf, just before the time that the *mao* touch-insensitive phenotype is first detected. This dose of tricaine abolished touch sensitivity when assessed at 32 hpf by exposing embryos to a series of tactile stimuli. By contrast, the frequency of cardiac contractions appeared unaffected compared with those of wild-type embryos. Furthermore, embryonic development continued and embryos appeared normal (Fig. 7A).

In tricaine-treated embryos, aat immunoreactivity remained continuous in RB peripheral processes (Fig. 7B, bottom) and resembled the pattern observed in both 36 hpf wild-type embryos and 48 hpf *mao* mutant embryos (Figs 1B, 3D). By contrast, the distribution of aat labeling within the peripheral processes of 60 hpf wild-type embryos was beaded (Fig. 7B, top). Tricaine treatment had no effect on the normal developmental changes of aat immunoreactivity within the spinal cord. These results indicate that tricaine treatment mimicked the effects of the *mao* mutation on developmental regulation of aat immunoreactivity in RB peripheral processes.

Counts of RB cells in tricaine-treated embryos revealed that the reduction of PCD was similar to that produced by the *mao* mutation (Fig. 8). By 72-78 hpf, RB somata were almost or completely absent from wild-type and *mao* sibling control embryos. By contrast, in tricaine-treated embryos or *mao* mutants, about half of the original RB cell population was still present (Fig. 9). Furthermore, the effects of the *mao* mutation and tricaine-treatment were first apparent at the same developmental stage, 60 hpf. At this time, both *mao* mutants and tricaine-treated embryos retain 10% more RB somata than sibling control or wild-type embryos.

DISCUSSION

While activity often acts to promote neuronal survival, we find that activity accelerates PCD of RB cells. RB cells acquire the ability to fire Na^+-dependent overshooting action potentials by

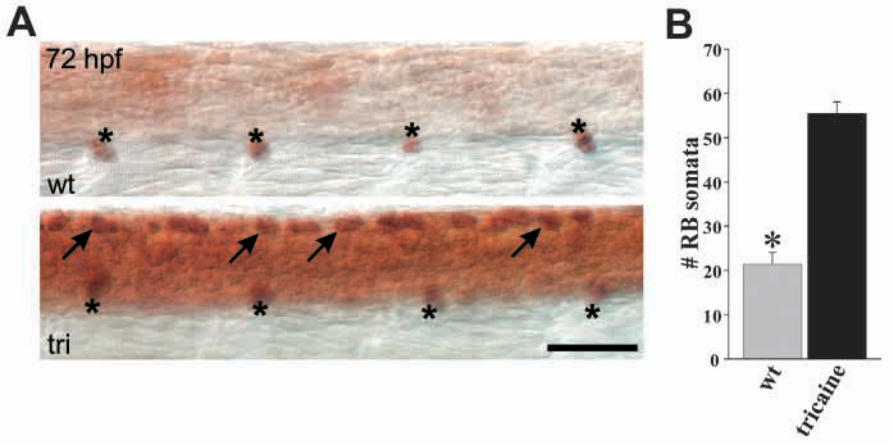

Fig. 8. Tricaine treatment phenocopies the effect of the *mao* mutation on Rohon-Beard cell death. (A) In lateral views of control (top) and tricaine-treated (bottom) embryos, HuA immunocytochemistry reveals dorsal root ganglia (asterisks). In addition, RB cells (arrows) are revealed in the tricaine-treated but not the control embryo. Scale bar: 40 μm. (B) RB cell counts indicate that there is a significant difference in the number of RB neurons present in 72 hpf tricaine-treated and control embryos ($P< 0.000001$; tricaine treated, $n=9$; untreated, $n=10$). Tricaine-treatment suppresses the normal loss of RB cells, as does the *mao* mutation.

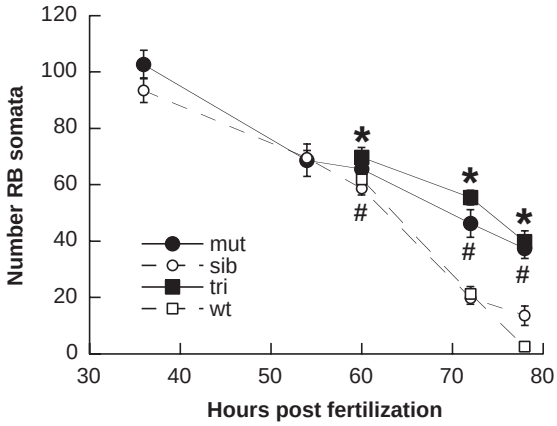

Fig. 9. Genetic and pharmacological silencing of Na^+ channels reduce RB cell death to the same extent. Numbers of RB somata are plotted as a function of time for wild-type (white squares), tricaine-treated (black squares), *mao* mutant (black circles), and *mao* sibling (white circles) embryos. At 36 and 54 hpf, the number of RB somata were similar for *mao* mutants and siblings. At 60 hpf, differences are first noted between the number of RB somata in *mao* sibling versus mutant embryos (*, P<0.05-0.0001). A similar ~10% difference is noted between the number of RB somata in wild-type and tricaine-treated embryos (#, P<0.05-0.000001). At subsequent stages, the differences between the number of RB somata between wild-type and *mao* sibling embryos versus tricaine-treated and *mao* mutant embryos increases. For example, at 72 hpf, there are approx. three times as many RB somata in *mao* mutant or tricaine-treated embryos versus *mao* sibling or wild-type embryos. At 78 hpf, there are approx. ten times as many RB somata in *mao* mutant and tricaine treated embryos versus either wild-type or sibling embryos. At all stages, the effects of the *mao* genetic lesion and pharmacological suppression on RB cell death are similar, and the numbers of RB somata in tricaine-treated and *mao* mutant embryos are similar. The number of embryos examined for each data point range between 5 and 10.

~1 dpf, as a result of developmental regulation of voltage-gated Na^+ current (Ribera and Nüsslein-Volhard, 1998). We blocked neural activity either genetically (*mao* mutant) or pharmacologically (tricaine). The effects of the *mao* mutation on RB Na^+ current are evident as early as 1 dpf, and lead to an obvious behavioral phenotype – touch insensitivity. For pharmacological suppression of Na^+ current, we treated embryos with tricaine beginning at 1 dpf, in order to mimic functionally and temporally the effects of the *mao* mutation. These manipulations reduced the number of TUNEL-positive RB neurons, redistribution of aat immunoreactivity in the periphery and the normal developmental loss of RB cell somata.

Three measures of programmed cell death in Rohon-Beard cells

Our results indicate that block of neural activity affects three properties of RB cells that are evident between 27-78 hpf. DNA fragmentation and cell body elimination are conventional markers of PCD. We propose that redistribution of acetylated-tubulin within the major peripheral processes of RB cells also reflects ongoing PCD and reports a stage that is between DNA fragmentation and cell body loss.

Discrete regions of swelling or beading form in neuronal processes as they degenerate either in pathological conditions or in response to injury (Ramon y Cajal, 1928; Delisle and Carpenter, 1984; Gold, 1987). Changes in the membrane cytoskeleton underlie the formation of the swellings (Ochs et al., 1996; Ochs et al., 1997; Hall et al., 1997b). Our data indicate that there is a reorganization of the membrane cytoskeleton of peripheral processes of dying RB cells. The redistribution of tubulin clearly precedes the eventual fragmentation of peripheral process and might be a prerequisite for process retraction.

Effects of the *mao* mutation on programmed cell death of Rohon-Beard cells are evident prior to dorsal root ganglion neuron differentiation

RB cells display an extreme form of normally occurring PCD, because they all die in zebrafish, as well as in several other species (Humphrey, 1944; Lamborghini, 1987; Kollros and Bovbjerg, 1997). RB cells exist only transiently and their function is assumed by later developing dorsal root ganglion neurons, raising the possibility that RB and dorsal root ganglion neurons compete for a common survival factor. However, RB cell death begins before dorsal root ganglion differentiation (Williams et al., 2000). Similarly, we find that the effects of the *mao* mutation on DNA fragmentation, an early index of PCD, are apparent as early as 36 hpf. At this time, dorsal root ganglion neurons are not yet detectable, even with immunological probes (Williams et al., 2000). These data suggest that the effects of activity blockade arise in Rohon-Beard cells rather than dorsal root ganglion cells.

Neural activity has diverse effects of neuronal survival and death

Neuronal activity can regulate cell survival. Often, activity promotes neuronal survival, and blockade of activity leads to an increase in developmental PCD. Genetic knockout of the voltage-gated Na^+ channel α-subunit, $Na_v1.2$, leads to profound CNS apoptosis, particularly in the neocortex and brainstem (Planells-Cases et al., 2000). Similarly, transmission blockade at the chick ciliary ganglion enhances cell death (Maderdrut et al., 1988). In these cases, activity appears to be required for survival of specific neuronal populations.

There are, however, examples of activity enhancing cell death, similar to what we report for zebrafish Rohon-Beard cells. A classic case is motoneuron cell death in the chick embryo. Here, block of synaptic transmission reduces the extent of normally occurring PCD (Pittman and Oppenheim, 1979; Oppenheim et al., 2000). Activity block also prevents death in the isthmo-optic nucleus (Pequignot and Clarke, 1992).

How does activity accelerate programmed cell death of Rohon-Beard cells?

Although it is clear that activity can have diverse effects on cell survival, little is known about the underlying mechanisms. With regard to the case of RB cells, we find that the *mao* mutation and pharmacological suppression of Na^+ current reduce the loss of RB somata to a similar extent (Fig. 9). However, neither manipulation of Na^+ current completely prevents death. Instead, the timecourse of PCD appears to be delayed (Fig. 9). Indeed, in 8 dpf *mao* mutants, no RB somata are detected (data not shown).

In wild-type embryos, the activation of the Na^+ current leads to elevation of intracellular Na^+, consequent depolarization,

followed by elevation of intracellular Ca^{2+}. Previous studies have demonstrated that elevations in intracellular Na^+ suffice to induce cell death. In rat superior cervical ganglion neurons, increases in intracellular Na^+ promote apoptosis; furthermore, cell death was not blocked by reduction of extracellular Ca^{2+} or buffering of intracellular Ca^{2+} (Koike et al., 2000). Cerebellar granule neurons also die in response to over-stimulation of Na^+ channels, even when Ca^{2+} channels and other routes of Ca^{2+} entry are blocked (Dargent et al., 1996). In worms, mutations in degenerin genes leads to constitutive activation of ion channels, elevation of intracellular Ca^{2+} and death of mechanosensory neurons (Hall et al., 1997a). The latter report is particularly intriguing given that RB cells also function as mechanosensory neurons. Perhaps, mechanosensory cells are more vulnerable to Na^+ overload.

Elevations of intracellular Ca^{2+} also suffice to promote cell death. For example, elevations of intracellular Ca^{2+} can activate Ca^{2+}-dependent proteolytic enzymes; these proteolytic enzymes cleave precursor forms of caspases, enzymes that mediate the cell death program (Salvesen and Dixit, 1997). Thus, elevations of intracellular Ca^{2+} might lead to activation of caspases and initiation of the cell death program.

Thus, it is possible that elevations in either intracellular Na^+ or Ca^{2+} might accelerate PCD of RB cells. Although our data do not allow us to distinguish between these possibilities, it is clear that both activity as well as neurotrophins regulate PCD of RB cells (Williams et al., 2000; this study). Whether and how these factors interact has yet to be determined.

We thank Dr Hans-Georg Frohnhöfer and the Tübingen Stockcenter for providing the *mao* mutant line; Ryan Heiser for expert fish maintenance; Dr Darren Gilmour for generous assistance with immunocytochemical procedures; Drs S. Rock Levinson and Robert Tanguay for use of microscopes and imaging systems; Drs Judith Eisen and Rosie Reyes for protocols; Drs Tom Finger, Joan Hooper, S. Rock Levinson, Robert Tanguay and Sukumar Vijayaraghavan for comments on the manuscript; and members of the laboratory for discussion. This work was supported by NIH grants F32-MH12748 (K. R. S.) and T32-NS07083 and NS38937 (A. B. R.).

REFERENCES

Abdelilah, S., Mountcastle-Shah, E., Harvey, M., Solnica-Krezel, L., Schier, A. F., Stemple, D. L., Malicki, J., Neuhauss, S. C., Zwartkruis, F., Stainier, D. Y. et al. (1996). Mutations affecting neural survival in the zebrafish *Danio rerio. Development* ***123***, 217-27.

Clarke, J. D. W., Hayes, B. P., Hunt, S. P. and Roberts, A. (1984). Sensory physiology, anatomy, and immunohistochemistry of Rohon-Beard neurons in embryos of *Xenopus laevis. J. Physiol.* ***348***, 511-525.

Clarke, P. G. (1985). Neuronal death during development in the isthmo-optic nucleus of the chick: sustaining role of afferents from the tectum. *J. Comp. Neurol.* **234**, 365-379.

Cowan, W. M., Fawcett, J. W., O'Leary, D. D. and Stanfield, B. B. (1984). Regressive events in neurogenesis. *Science* **225**, 1258-1265.

Daly, F. J. and Sandell, J. H. (2000). Inherited retinal degeneration and apoptosis in mutant zebrafish. *Anat. Rec.* **258**, 145-155.

Dargent, B., Arsac, C., Tricaud, N. and Couraud, F. (1996). Activation of voltage-gated sodium channels in cultures of cerebellar granule cells induces neurotoxicity that is not mediated by glutamate release. *Neuroscience* **73**, 209-216.

Delisle, M. B. and Carpenter, S. (1984). Neurofibrillary axonal swellings and amyotrophic lateral sclerosis. *J. Neurol. Sci.* **63**, 241-250.

Derer, P. and Derer, M. (1990). Cajal-Retzius cell ontogenesis and death in mouse brain visualized with horseradish peroxidase and electron microscopy. *Neuroscience* **36**, 839-856.

Frazier, D. T. and Narahashi, T. (1975). Tricaine (MS-222): effects on ionic conductances of squid axon membranes. *Eur. J. Pharm.* **33**, 313-317.

Frotscher, M. (1997). Dual role of Cajal-Retzius cells and reelin in cortical development. *Cell Tiss. Res.* **290**, 315-322.

Furutani-Seiki, M., Jiang, Y. J., Brand, M., Heisenberg, C. P., Houart, C., Beuchle, D., van Eeden, F. J., Granato, M., Haffter, P., Hammerschmidt, M. et al. (1996). Neural degeneration mutants in the zebrafish, *Danio rerio. Development* **123**, 229-239.

Ghosh, A., Carnahan, J. and Greenberg, M. E. (1994). Requirement for BDNF in activity-dependent survival of cortical neurons. *Science* **263**, 1618-1623.

Gold, B. G. (1987). The pathophysiology of proximal neurofilamentous giant axonal swellings: implications for the pathogenesis of amyotrophic lateral sclerosis. *Toxicology* **46**, 125-139.

Granato, M., van Eeden, F. J., Schach, U., Trowe, T., Brand, M., Furutani-Seiki, M., Haffter, P., Hammerschmidt, M., Heisenberg, C. P., Jiang, Y. J. et al. (1996). Genes controlling and mediating locomotion behavior of the zebrafish embryo and larva. *Development* **123**, 399-413.

Grunwald, D. J., Kimmel, C. B., Westerfield, M., Walker, C. and Streisinger, G. (1988). A neural degeneration mutation that spares primary neurons in the zebrafish. *Dev. Biol.* **126**, 115-128.

Haffter, P., Granato, M., Brand, M., Mullins, M. C., Hammerschmidt, M., Kane, D. A., Odenthal, J., van Eeden, F. J. M., Jiang, Y.-J., Heisenberg, C.-P. et al. (1996). The identification of genes with unique and essential functions in the development of the zebrafish, *Danio rerio*. *Development* **123**,1-36.

Hall, D. H., Gu,G., Garcia-Anoveros, J., Gong, L., Chalfie, M. and Driscoll, M. (1997a). Neuropathology of degenerative cell death in Caenorhabditis elegans. *J. Neurosci.* **17**, 1033-1045.

Hall, G. F., Yao, J., Selzer, M. E. and Kosik, K. S. (1997b). Cytoskeletal changes correlated with the loss of neuronal polarity in axotomized lamprey central neurons. *J. Neurocytol.* **26**, 733-753.

Henion, P. D., Raible, D. W., Beattie, C. E., Stoesser, K. L., Weston, J. A. and Eisen, J. S. (1996). Screen for mutations affecting development of zebrafish neural crest. *Dev. Genet.* **18**, 11-17.

Hensey, C. and Gautier, J. (1998). Programmed cell death during *Xenopus* development: a spatio-temporal analysis. *Dev. Biol.* **203**, 36-48.

Humphrey, T. (1944). Primitive neurons in the embryonic human central nervous system. *J. Comp. Neurol.* **81**, 1-45.

Kaplow, L. S. (1974). Substitute for benzidine in myeloperoxidase stains. *Am. J. Clin. Path.* **63**, 451.

Kerr, J. F. R., Wyllie, A. H. and Currie, A. R. (1972). Apoptosis: a basic biological phenomenon with wide-ranging implications in tissue kinetics. *Br. J. Cancer* **26**, 239-257.

Kimmel, C. B., Ballard, W. W., Kimmel, S. R., Ullamann, B. and Schilling, T. F. (1995). Stages of embryonic development of the zebrafish. *Dev. Dyn.* **203**, 253-310.

Koike, T., Tanaka, S., Oda, T. and Ninomiya, T. (2000). Sodium overload through voltage-dependent Na+ channels induces necorosis and apoptosis of rat superior cervical ganglion cells in vitro. *Br. Res. Bull.* **51**, 345-355.

Kollros, J. J. and Bovbjerg, A. M. (1997). Growth and death of Rohon-Beard cells in Rana pipiens and Ceratophrys ornata. *J. Morphol.* **232**, 67-78.

Kuida, K., Zheng, T. S., Na, S., Kuan, C., Yang, D. Kurasuyama, H., Rakic, P. and Flavell, R. A. (1996). Decreased apoptosis in the brain and premature lethality in CPP32-deficient mice. *Nature* **384**, 368-372.

Lamborghini, J. E. (1987). Disappearance of Rohon-Beard neurons from the spinal cord of larval Xenopus laevis. *J. Comp. Neurol.* **264**, 47-55.

Larmet, Y., Dolphin, A. C., And Davies, A. M. (1992). Intracellular calcium regulates the survival of early sensory neurons before they become dependent on neurotrophic factors. *Neuron* **9**, 563-574.

Lievremont, J. P., Sciorati, C., Morandi, E., Paolucci, C., Bunone, G., Della Valle, G., Meldolesi, J. and Clementi, E. (1999). The p75(NTR)-induced apoptotic program develops through a ceramide-caspase pathway negatively regulated by nitric oxide. *J. Biol. Chem.* **274**, 15466-15472.

Maderdrut, J. L., Oppenheim, R. W. and Prevette, D. (1988). Enhancement of naturally occurring cell death in the sympathetic and parasympathetic ganglia of the chicken embryo following blockade of ganglionic transmission. *Brain Res.* **444**, 189-194.

Marusich, M. F., Furneaux, H. M., Henion, P. D. and Weston, J. A. (1994). Hu neuronal proteins are expressed in proliferating neurogenic cells. *J. Neurobiol.* **25**, 143-155.

Metcalfe, W. K., Myers, P. Z., Trevarrow, B., Bass, M. B. and Kimmel, C. B. (1990). Primary neurons that express the L2/HNK-1 carbohydrate during early development in the zebrafish. *Development* **110**, 491-504.

Ochs, S., Pourmand, R. and Jersild, R. A. (1996). Origin of the beading constrictions at the axolemma: presence in unmyelinated axons and after beta, beta'-iminodipropionitrile degradation of the cytoskeleton. *Neuroscience* **70**, 1081-1096.

Ochs, S., Pourmand, R., Jersild, R. A. and Friedman, R. N. (1997). The origins and nature of beading: a reversible transformation of nerve fibers. *Prog. Neurobiol.* **52**, 391-426.

Oppenheim, R. W. (1991). Cell death during development of the nervous system. *Annu. Rev. Neurosci.* **14**, 453-501.

Oppenheim, R. W., Prevette, D., D'Costa, A., Wang, S., Houenou, L. J. and McIntosh, J. M. (2000). Reduction of neuromuscular activity is required for the rescue of motoneurons from naturally occurring cell death by nicotinic-blocking agents. *J. Neurosci.* **20**, 6117-24.

Pequignot, Y. and Clarke, P. G. (1992). Changes in lamination and neuronal survival in the isthmo-optic nucleus following the intraocular injection of tetrodotoxin in chick embryos. *J. Comp. Neurol.* **321**, 336-350.

Pittman, R. and Oppenheim, R. (1979). Cell death of motoneurons in the chick embryo spinal cord. IV. Evidence that a functional neuromuscular interaction is involved in the regulation of naturally occurring cell death and the stabilization of synapses. *J. Comp. Neurol.* **187**, 425-46.

Planells-Cases, R., Caprini, M., Zhang, J., Rockenstein, E. M., Rivera, R. R., Murre, C., Masliah, E. and Montal, M. (2000). Neuronal death and perinatal lethality in voltage-gated sodium channel alpha(II)-deficient mice. *Biophys. J.* **78**, 2878-2891.

Ramon y Cajal, S. (1928). *Degeneration and Regeneration of the Nervous System* (ed. R. M. May). New York: Hafner.

Reyes, R. (2000). Development and death of zebrafish Rohon-Beard spinal sensory neurons. In *Department of Biology*, pp. 1-69. Eugene, OR: University of Oregon.

Ribera, A. B. and Nüsslein-Volhard, C. (1998). Zebrafish touch-insensitive mutants reveal an essential role for the developmental regulation of sodium current. *J. Neurosci.* **18**, 9181-9191.

Saint-Amant, L. and Drapeau, P. (1998). Time course of the development of motor behaviors in the zebrafish embryo. *J. Neurobiol.* **37**, 622-632.

Saint-Amant, L. and Drapeau, P. (2000). Motoneuron activity patterns related to the earliest behavior of the zebrafish embryo. *J. Neurosci.* **20**, 3964-3972.

Salvesen, G. S. and Dixit, V. M. (1997). Caspases: intracellular singalling by proteolysis. *Cell* **91**, 443-446.

Schinder, A. F. and Poo, M.-m. (2000). The neurotrophin hypothesis for synaptic plasticity. *Trends Neurosci.* **23**, 639-645.

Searle, J., Kerr, J. F. R. and Bishop, C. J. (1982). Necrosis and apoptosis: distinct modes of cell death with fundamentally different significance. *Pathol. Annu.* **17**, 229-259.

Soffe, S. R. (1991). Triggering and gating of motor responses by sensory stimulation: behavioural selection in Xenopus embryos. *Proc. R. Soc. London* **246**, 197-203.

Wang, G. K., Mok, W. M. and Wang, S. Y. (1994). Charged tetracaine as an inactivation enhancer in batrachotoxin-modified Na+ channels. *Biophys. J.* **67**, 1851-1860.

Westerfield, M. (1994). *The Zebrafish Book*. Eugene, OR: University of Oregon Press.

Williams, J. A., Barrios, A., Gatchalian, C., Rubin, L., Wilson, S. W. and Holder, N. (2000). Programmed cell death in zebrafish Rohon Beard neurons is influenced by TrkC1/NT-3 signaling. *Dev. Biol.* **226**, 220-230.